ARTICLE

Oxidative Dehydrogenation of Alkanes using Oxygen-Permeable Membrane Reactor

Rui-qiang Yan[a], Wei Liu[c], Chun-lin Song[b*]

a. Department of Materials Engineering, Taizhou University, Taizhou 318000, China
b. Faculty of Materials and Energy, Southwest University, Chongqing 400715, China
c. CAS Key Lab Mat Energy Convers, Department of Materials Science and Engineering, University of Science and Technology of China, Hefei 230026, China

(Dated: Received on July 1, 2014; Accepted on September 9, 2014)

The oxidative dehydrogenation (ODH) reactions of ethane and propane were investigated in a catalytic membrane reactor, incorporating oxygen-permeable membranes based upon $La_2Ni_{0.9}V_{0.1}O_{4+\delta}$ or $Ba_{0.5}Sr_{0.5}Co_{0.8}Fe_{0.2}O_{3-\delta}$. As a compromise between the occurrence of a measureable oxygen flux and excessive homogenous gas phase reactions, the measurements were conducted at an intermediate temperature, either at 550 or 650 °C. The results show the dominating role of the oxygen flux across the membrane and available sites at the membrane surface in primary activation of the alkane and, hence, in achieving high alkane conversions. The experimental data of ODH of propane and ethane on both membrane materials can be reconciled on the basis of Mars-van Krevelen mechanism, in which the alkane reacts with lattice oxygen on the membrane surface to produce the corresponding olefin. It is further demonstrated that the oxygen concentration in the gas phase and on the membrane surface is crucial for determining the olefin selectivity.

Key words: Oxidative dehydrogenation, Membrane reactor, Oxygen-permeable membrane

I. INTRODUCTION

The major transformation techniques of light alkanes into corresponding olefins include steam cracking, fluid catalytic cracking, and catalytic dehydrogenation [1−4]. Over the past few years, oxidative dehydrogenation (ODH) of alkanes has gained much interest [5−11]. While ODH is exothermal, both catalytic dehydrogenation and thermal cracking are endothermal [6]. In the present work, we are primarily concerned with heterogeneous ODH, using a redox-active oxide catalyst, rather than the homogenous gas phase reaction in the presence of gaseous oxygen. The former is consistent with a redox cycle known as the Mars-van Krevelen mechanism [6, 12]. In the reduction cycle, lattice oxygen abstracts hydrogen from the alkane. The resulting alkyl species is desorbed as an olefin, while the surface hydroxyl groups formed during reaction recombine and are desorbed as water, leaving a surface oxygen vacancy (and a reduced metal center) behind. In the oxidation cycle, the catalyst is re-oxidized. Usually, this is done by gas phase oxygen.

The selective oxidation reaction can occur either with insertion of oxygen, such as in the formation of acrolein from propane, or without insertion of oxygen, such as in oxidative dehydrogenation, *e.g.*, the formation of propylene from propane. The importance of lattice oxygen in selective oxidation reactions of hydrocarbons has already been recognized as early as in the 1950s [13]. How to re-oxidize the catalyst in order to complete the Mars-van Krevelen redox cycle is, though relevant, of second concern, and is further discussed below. The metal-oxygen bond strength of active oxygen sites at the catalyst surface needs to be of intermediate strength [12]. If the metal-oxygen bond strength is too strong, no reaction at all will occur, if too weak, over-oxidation might occur, leading to combustion products CO_x. It is thus required that the oxide catalyst has an appropriate host structure, containing redox active metal cations, and is able to adopt oxygen-deficient stochiometries without a collapse of the structure. Favorable catalysts are usually multi-metal oxides with, *e.g.*, a scheelite, fluorite or perovskite structure, often containing vanadium or molybdenum as one of the active constituents [5, 8, 12].

To avoid the presence of unselective weakly-bonded adsorbed oxygen species (*e.g.* O_2^-, O_2^{2-}, O^-) at the surface, oxygen concentrations in the gas phase need to be minimized during reaction. Several approaches have been pursued to separate reduction and oxidation steps compliant with Mars-van Krevelen type of kinetics, either in time by periodic operation of the reaction by alternate feeding of alkane and oxygen [6], or spatially by using moving bed technology [14] or a catalytic membrane reactor [9, 15−19]. In the latter, a mixed oxide

*Author to whom correspondence should be addressed. E-mail: chunlinsong@swu.edu.cn, Tel.: +86-18883327083

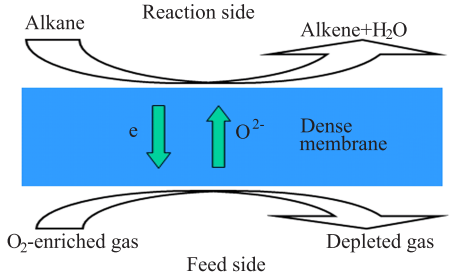

FIG. 1 Schematics of catalytic membrane reactor.

ionic-electronic conducting membrane, endowed with suitable catalytic properties or modified with a suitable catalyst, is employed. The membrane facilitates a continuous and controlled flux of oxide ions to the permeate side exposed to the alkane feed, as illustrated in Fig.1 [17, 19]. The oxygens arrive at the surface via solid-state diffusion exclusively. Accumulation of oxygen in the gas phase can be avoided by matching the oxygen flux through the membrane with the rate of consumption of oxygen by the selective oxidation reaction at the immediate membrane surface.

Wang *et al.* [17] reported selectivity of 80.1% towards ethylene at ethane conversion of 84.2%, using a catalytic membrane reactor made of $Ba_{0.5}Sr_{0.5}Co_{0.8}Fe_{0.2}O_{3-\delta}$ (BSCF), at 800 °C, whereas selectivity and conversion of 53.7% and 83.6%, respectively, were obtained using BSCF powder in a conventional fixed-bed reactor. When propane was used as a reactant, selectivity of 23.9% towards propylene at conversion of 71.8% was obtained at 750 °C [19]. In a similar study of ODH of ethane to ethylene, Rebeilleau-Dassonneville *et al.* [16] observed substantial formation of hydrogen as a by-product, indicating that the reaction significantly proceeds via gas phase dehydrogenation. It is required to clarify the role of the membrane, where it should be noted that both selectivity and yield are found to be enhanced by application of a surface catalyst at the permeate side of the BSCF membrane [16].

In this work, we explored the mechanism of oxidative dehydrogenation of alkanes in the oxygen-permeable membrane reactor. Catalytic membrane reactors, made of either $La_2Ni_{0.9}V_{0.1}O_{4+\delta}$ (LNV10) or BSCF, were exploited for ODH of propane and ethane. The influence of the catalytic membrane on the ODH reaction was studied. As a compromise between a measurable oxygen flux and occurrence and extent of the gas phase reactions, the measurements were conducted at an intermediate temperature, either 550 or 650 °C, to minimize the extent of the gas phase reaction.

II. EXPERIMENTS

A. Membrane preparation and characterization

Powders of LNV10 and BSCF were prepared by thermal decomposition of precursor complexes derived from a mixed solution, containing the corresponding metal ions in the appropriate stoichiometry, using ethylenediaminetetraacetic (EDTA) as complexing agent. The vanadium-containing solution was prepared by dissolving V_2O_5 in diluted HNO_3. Metal nitrates were used for preparing the other solutions. The powders obtained were calcined in air for 10 h, at 1050 and 950 °C for LNV10 and BSCF, respectively. After calcination, the powder was ball-milled in acetone for 5 h. Phase purity of the powders was checked by X-ray diffraction, using a Philips PANalytical PW1830 diffractometer. Powders of LNV10 were pressed into either green tubes or discs via cold isostatic pressing at 400 MPa, and subsequently sintered in air at 1420 ° C for 10 h, using heating and cooling rates of 3 °C/min. Similarly, BSCF powders were pressed into discs and sintered at 1220 °C. The relative density of the dense ceramics was higher than 95%. Surface of the membranes were carefully polished by hand using 240-mesh SiC grinding paper.

Oxygen permeation through the LNV10 disc membrane (0.97 mm thickness) was measured in the range of 575−700 °C. Soda lime silicate glass (AR-glass) rings were used for sealing of the disc into the reactor. After sealing, synthetic air and high purity helium were fed to opposite sides of the membrane at flow rates of 100 and 10 mL/min, respectively. The effluent gas was analyzed by on line gas chromatography (Varian CP 4900 equipped with molecular sieve 5A PLOT and PoraPLOT Q columns). The gas chromatograph was calibrated using standard gas mixtures (O_2, N_2 balanced with He). Oxygen leakage, due to imperfect sealing, was evaluated by measuring the nitrogen concentration in the effluent gas. Permeation data were corrected for oxygen leakage, using the corresponding nitrogen concentration. Corrections were less than 1% of the total oxygen concentration in the effluent gas.

B. Catalytic experiments

ODH of propane was studied, at 650 °C, using a tubular LNV10 membrane reactor of length 33 mm, and with outside and inside diameters of 6 and 4.1 mm, respectively. A gas mixture of oxygen balanced with nitrogen (∼100 mL/min), having oxygen partial pressures in the range of 0.1−0.8 atm, was fed to the feed side, while 10% propane balanced with helium (∼10 mL/min) was fed to the reaction (permeate) side of the LNV10 membrane.

Similarly, studies of ODH of ethane and propane, using BSCF disc membranes, were conducted, at either 550 or 650 °C. The thickness of the membranes varied between 0.8 and 1.0 mm, while the effective membrane area at the reaction side was about ∼0.8 cm^2. For ODH of propane, 10% propane balanced with helium (∼10 mL/min) was swept along the reaction side, feeding nitrogen (∼100 mL/min) on the opposite side of the membrane. Next, the nitrogen was diluted with

DOI:10.1063/1674-0068/27/06/690-696

oxygen (∼100 mL/min) to give oxygen partial pressures in the range of 0.02−0.4 atm. Prior to experiment, the membrane was pre-equilibrated for 5 h, using nitrogen (∼100 mL/min) and helium (∼10 mL/min) as sweep gases along both sides of the membrane. For ODH of ethane, oxygen balanced with nitrogen (∼100 mL/min), having an oxygen partial pressure of 0.1−0.8 atm, was fed to the feed side, while diluted ethane (∼10 mL/min), in the range of 24%−76% in helium, was fed to the reaction side of the BSCF membrane.

To investigate thermal cracking and/or dehydrogenation of the alkanes in the gas phase, experiments were carried out, using either a quartz tube or discs, replacing tubular and planar membranes, respectively, and keeping all other conditions similar to those as used in the membrane reactor experiments. These experiments, referred to as blank experiments, were carried out both in the absence and presence of gaseous oxygen.

Reactor effluents were analyzed using on line gas chromatography, as specified above. All reactant gases passed through an ice-bath condenser before injection into the gas chromatograph. The absence of nitrogen in the effluents was taken as evidence that no leakage occurred through the membrane or glass seal.

Conversions and selectivities were calculated based on the carbon balance [19]. The conversion was calculated from the following equation:

$$C = 1 - \frac{nY_{\mathrm{C}_n\mathrm{H}_{2n+2}}}{\sum m_i Y_i} \tag{1}$$

where m_i and Y_i are the number of carbon atoms and molar fraction of the i-th carbon-containing product, respectively. The selectivity towards the i-th carbon-containing product was calculated from

$$S_i = \frac{m_i Y_i}{\sum m_i Y_i - nY_{\mathrm{C}_n\mathrm{H}_{2n+2}}} \tag{2}$$

For all catalytic tests, the carbon balance was within 100%±1%.

III. RESULTS AND DISCUSSION

A. Characterization of membrane materials

The XRD powder diffraction pattern of LNV10 is presented in Fig.2. Like that of its parent La_2NiO_4, the pattern of LNV10 can be indexed on the basis of a tetragonal unit cell, with cell parameters a=3.873(2) Å and c=12.659(2) Å. The diffraction pattern of BSCF (not shown) could be indexed on the basis of a simple cubic perovskite structure. In both cases, no evidence was found for the presence of phase impurities or second phase formation.

Figure 3 shows oxygen permeation measurements results of LNV10 in this work, results for BSCF reported in Ref.[20] are also shown for comparison. From these data it is apparent that, at the moderate temperatures covered experimentally, oxygen transport in LNV10 is much lower than in BSCF. A value of 164 kJ/mol was calculated for the activation energy for oxygen permeation through LNV10.

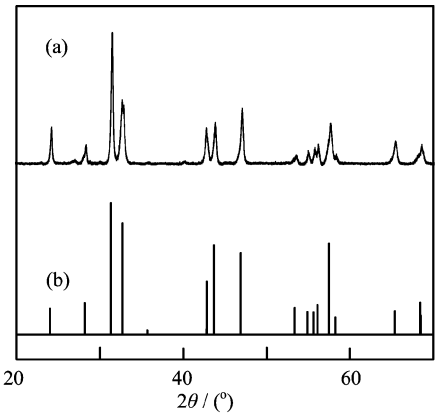

FIG. 2 X-ray powder diffraction pattern of (a) LNV10 collected at room temperature and (b) the calculated pattern.

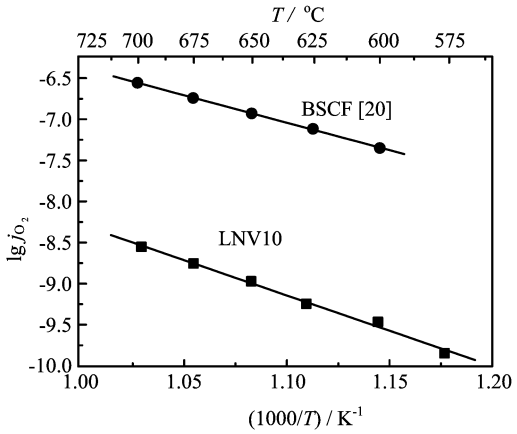

FIG. 3 Oxygen permeation flux (j_{O_2}) through a disc LNV10 membrane with thickness 0.97 mm. Synthetic air was used as feed gas (100 mL/min), while helium was used as purge gas (10 mL/min) at the permeate side of the membrane. Also shown are data for a BSCF membrane with thickness of 1.5 mm from Ref.[20].

B. ODH of propane using catalytic membrane reactors

Quantifiable reaction products observed when propane passed through the tubular LNV10 membrane reactor were H_2, CH_4, CO, CO_2, H_2O, C_2H_4, C_2H_6 and C_3H_6. Figure 4 shows the distribution of products, at 650 °C, while maintaining p_{O_2} of 0.8 atm at the feed side of the membrane. Also shown in the figure are the corresponding data from pyrolysis experiments in an empty reactor (referred to as blank experiments). It

DOI:10.1063/1674-0068/27/06/690-696

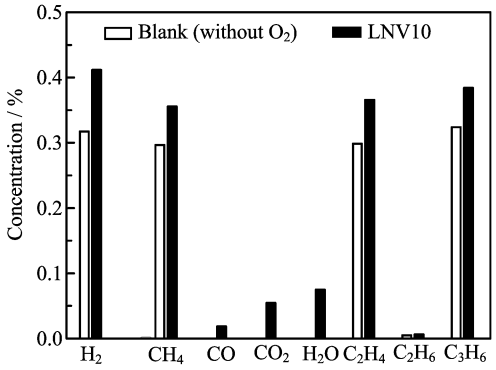

FIG. 4 Product distribution in ODH of propane, at 650 °C, from experiments using the LNV10 membrane reactor. Reactant side: 10%C_3H_8 (10 mL/min), feed side: p_{O_2}=0.80 atm. Also shown are corresponding results of propane pyrolysis experiments (blank), at 650 °C, performed in an empty quartz reactor.

is clear that under the conditions of the experiments there is a significant contribution from gas phase reactions. Besides H_2O, combustion products CO_x are formed when oxygen is fed to propane via the LNV10 membrane.

In Fig.5(a), the product concentrations are plotted against the oxygen flux. The latter was varied by maintaining different oxygen partial pressures, in the range of 0.1−0.8 atm, at the feed side of the membrane during the experiments. The results show that the oxygen concentration at the reaction side remains virtually zero, while the formation of all products, including H_2O and CO_x, increases with increasing the oxygen flux.

As shown in Fig.5(b), the conversion of propane increases concomitantly from 6.3% to 7.8%, without a significant change in the propylene selectivity. In the range of the experiments, the latter slightly decreases from 51.8% to 49.5%. The emerging picture is that, at given experimental conditions, the oxygen flux through LNV10 is too small, while the gas phase reactions are too prominent, demonstrating the determining role of lattice oxygen on propylene selectivity.

Figure 6 shows the reaction products, at 550 °C, upon passing propane through the BSCF membrane reactor, while maintaining p_{O_2}=0.05 atm at the feed side of the membrane. Reaction products include H_2, CH_4, CO, CO_2, H_2O, C_2H_4, C_2H_6, and C_3H_6. Also shown in Fig.6 are data of thermal pyrolysis and ODH of propane, at 550 °C, in an empty reactor (referred to as blank experiments, without and with O_2, respectively).

It is generally accepted that the homogeneous gas phase reactions during ODH of alkanes occur via a free-radical chain mechanism [21]. Oxygen may be involved in the initiation reaction, *e.g.*, through hydrogen abstraction from the alkane. Also, thermal cracking may generate free radical species, causing a large variety of successive elementary chain reactions [21]. The data presented in Fig.6 suggest that, at given experimental

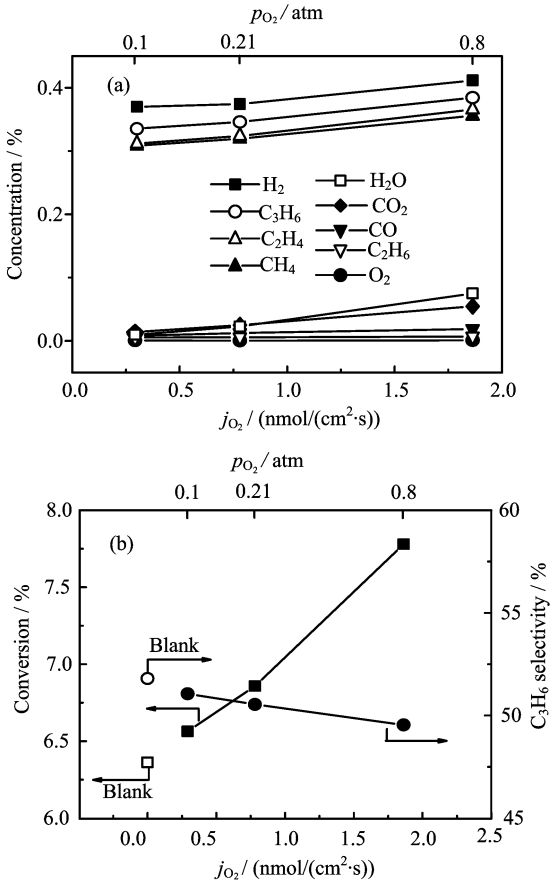

FIG. 5 Catalytic performance of the LNV10 membrane reactor in ODH of propane, at 650 °C, as a function of the oxygen permeation flux (j_{O_2}). (a) Product distribution and (b) conversion and propylene selectivity. Reactant side: 10%C_3H_8 (10 mL/min). Oxygen partial pressures maintained at the feed side of the membrane are indicated in the figures. Also indicated in (b) are corresponding results from propane pyrolysis experiments (blank), at 650 °C, performed in an empty quartz reactor.

conditions, amongst which the absence of a catalyst is considered important, molecular oxygen acts as a scavenger of free radicals. Compared to the data from pyrolysis experiments, addition of oxygen to the propane stream is found to lower propane conversion. The conversion is further lowered upon increasing the oxygen concentration in the gas phase, as can be judged from the data presented in Table I. Under the conditions of the experiments with O_2, the oxygen consumption by gas phase reactions is limited. As seen in Fig.6., free, *i.e.*, unreacted, oxygen can be still detected, while only limited oxygen is traced back in the form of CO_2, but none in the form of H_2O. The situation alters when oxygen is supplied to the propane stream via the BSCF membrane. Although free oxygen can still be detected in the gas phase, significantly enhanced conversion to olefins (C_2H_4, C_3H_6) is found.

The data shown in Fig.6 emphasize on the catalytic

DOI:10.1063/1674-0068/27/06/690-696

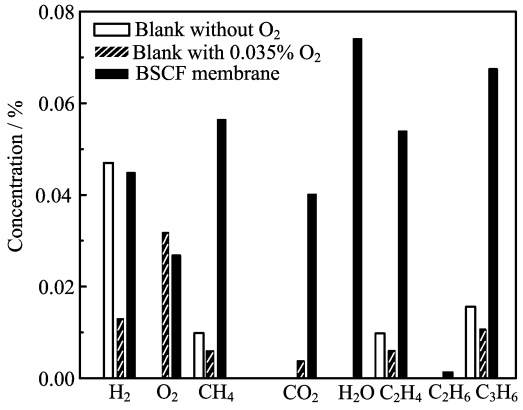

FIG. 6 Product distribution in ODH of propane, at 550 °C, from experiments using the BSCF membrane reactor. Reactant side: 10%C_3H_8 (10 mL/min), feed side: p_{O_2}=0.05 atm. Also shown are corresponding data of thermal pyrolysis experiments (blank, without O_2) and ODH of propane (blank, with O_2), at 550 °C, performed in an empty quartz reactor.

TABLE I Conversion and C_3H_6 selectivity in thermal pyrolysis and ODH of propane, at 550 °C, performed in an empty quartz reactor without or with different content of O_2.

Inlet gas composition	Conversion/%	Selectivity/%
10%C_3H_8/He	0.25	61.4
0.035%O_2/8.64%C_3H_8/He	0.21	59.5
0.070%O_2/7.20%C_3H_8/He	0.15	63.6

role of BSCF in the dehydrogenation of propane. It is assumed that propyl radicals are generated at the BSCF surface involving a mechanism in which lattice oxygen is responsible for C−H bond activation, and one which is consistent with a Mars-van Krevelen redox mechanism [6]. The propyl radical is desorbed as olefin with concomitant formation of H_2O. The presence of reaction products CH_4 and C_2H_4, however, indicates that under the conditions of the experiments gas phase reactions are active. The enhanced formation of CO_2, relative to the blank experiments in an empty reactor, *i.e.* in the presence of oxygen, suggests that CO_2 is essentially formed at the BSCF surface. Increasing the oxygen flux, by maintaining a higher oxygen partial pressure at the feed side of the BSCF membrane in a series of experiments, from p_{O_2}=0.02 atm to p_{O_2}=0.40 atm, as shown in Fig.7, increases production of CO_2, but lowers conversion of propane. The propylene selectivity is only slightly reduced. It thus emerges that the membrane-assisted catalytic conversion of propane is an interplay between operating constraints (like the number of sites at the surface, residence time, feed concentrations, *etc.*), the oxygen flux, and the occurrence and extent of homogenous gas phase reactions. A distinct oxygen flux is required to achieve the desired conversion of the alkane into the corresponding olefin. A too high

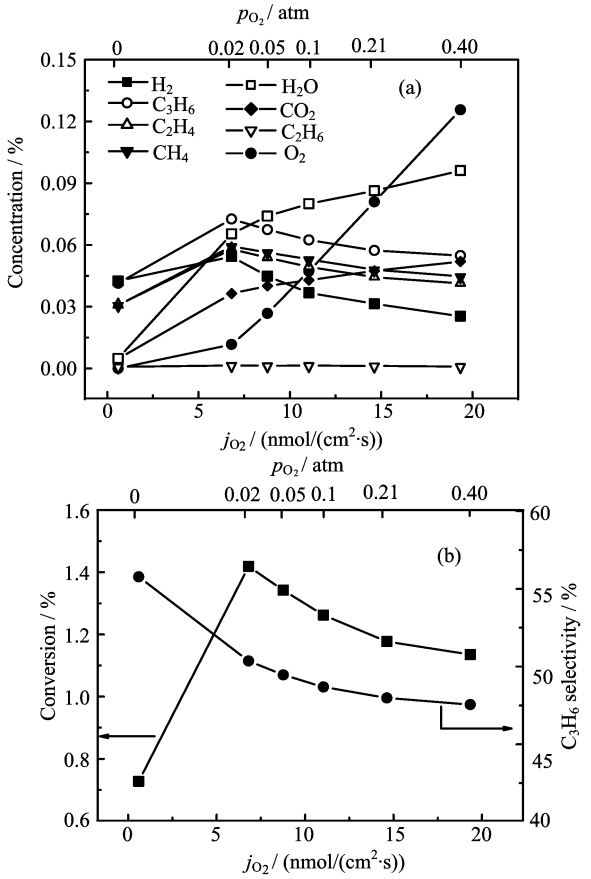

FIG. 7 Catalytic performance of the BSCF membrane reactor in ODH of propane, at 550 °C, as a function of the oxygen permeation flux. (a) Product distribution and (b) conversion and propylene selectivity. Reactant side: 10%C_3H_8 (10 mL/min).

oxygen flux, however, leads to (i) unselective weakly-bonded adsorbed oxygen species, oxidizing alkyl radicals at the catalytic membrane surface, thereby producing CO_2, and (ii) increases the concentration of gaseous oxygen, limiting the extent of the gas phase reactions.

C. ODH of ethane using the BSCF catalytic membrane reactor

The catalytic performance of the BSCF membrane reactor was conducted, at 650 °C, in ODH of ethane. Typical results obtained upon passing 40.5% ethane, balanced with helium, through the reactor, while maintaining p_{O_2}=0.8 atm at the feed side of the BSCF membrane, are shown in Fig.8.

Quantifiable reaction products at the exit of the reactor were H_2, CH_4, CO, CO_2, H_2O, and C_2H_4. Under the conditions of the experiments, ethane conversion was 6.09% with ethylene selectivity of 87.7%. Results of thermal pyrolysis experiments (blank experiments) carried out in an empty reactor are shown in Table II.

DOI:10.1063/1674-0068/27/06/690-696

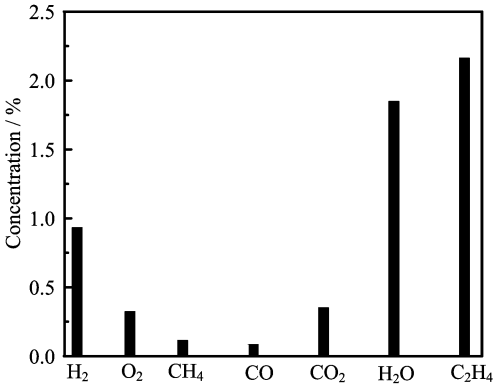

FIG. 8 Product distribution in ODH of ethane, at 650 °C, from experiments using the BSCF membrane reactor. Reactant side: 40.5%C_2H_6 (10 mL/min), feed side: p_{O_2}=0.80 atm.

TABLE II Conversion and C_2H_4 selectivity derived from ethane pyrolysis experiments with different feed concentration of C_2H_6, at 650 °C, performed in an empty quartz reactor.

C_2H_6/%	Conversion/%	C_2H_4 selectivity/%
25.3	0.42	99.6
42.9	0.41	99.5
61.6	0.39	99.5
81.0	0.37	99.4

It is seen that the corresponding ethylene selectivities are close to 100%, albeit that these are at low ethane conversions in the range of 0.37%−0.42%, obtained using different feed concentrations of ethane (Table II). In accord with the data presented in Fig.9, ethane conversion is found to increase pronouncedly if oxygen is fed via the BSCF membrane to the reaction side where the ethane is passed. The loss in ethylene selectivity observed in the membrane experiment, relative to that obtained during thermal pyrolysis in the empty reactor, is explained by the fact that the oxygen flux exceeds the rate of oxygen consumption by the catalytic reaction at the membrane surface. The presence of weakly adsorbed oxygen species in conjunction with gas phase oxygen lowers the overall ethylene selectivity. It is also confirmed by the results from measurements, in which either the inlet concentration of ethane was varied, *i.e.*, at constant p_{O_2} at the feed side of the BSCF membrane, as listed in Table III, or those in which the p_{O_2} at the feed side of the BSCF membrane was varied, *i.e.*, at constant inlet concentration of ethane, as shown in Fig.9. Both data sets demonstrate that the ethylene selectivity increases when the oxygen flux and rate of oxygen consumption by the catalytic reaction are better in balance.

On the whole, the oxygen concentration both in the gas phase and on the surface of the catalyst membrane is crucial for determining the selectivity for ODH of ethane and propane.

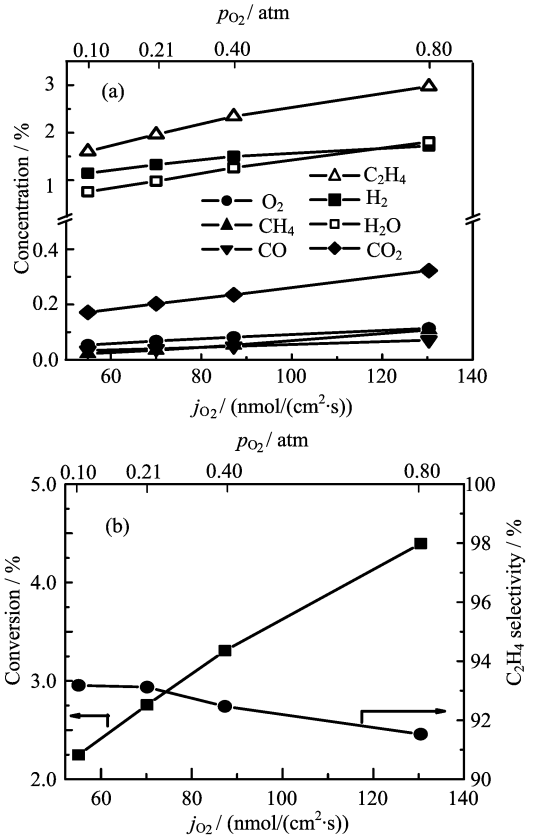

FIG. 9 Catalytic performance of the BSCF membrane reactor in ODH of ethane, at 650 °C, as a function of the oxygen permeation flux. (a) Product distribution and (b) conversion and ethylene selectivity. Reactant side: 73.9%C_2H_6 (10 mL/min). Oxygen partial pressures maintained at the feed side of the membrane are indicated in the figures.

TABLE III Catalytic performance of the BSCF membrane reactor in ODH of ethane, at 650 °C, using different inlet concentrations of ethane (10 mL/min). Feed side: p_{O_2}=0.80 atm. Also given are the gas phase oxygen concentrations measured at the reaction side of the membrane.

C_2H_6/%	Conversion/%	Selectivity/%	O_2/%
24.3	3.48	78.8	1.18
40.5	6.09	87.7	0.32
57.2	5.31	90.1	0.17
73.9	4.40	91.5	0.11

IV. CONCLUSION

In summary, the results show the dominating role of the oxygen flux across the membrane and available sites at the membrane surface in primary activation of the alkane and, hence, in achieving high alkane conversions. The results of ODH of propane and ethane on

DOI:10.1063/1674-0068/27/06/690-696

both membrane materials used in this work can be reconciled on the basis of Mars-van Krevelen type of kinetics, in which the alkane reacts with lattice oxygen on the membrane surface to produce the corresponding olefin. As expected, the oxygen concentration in the gas phase and the presence of weakly-bonded oxygen species on the membrane surface are crucial for determining the residual olefin selectivity. The latter emphasize on the paramount importance to carefully match the oxygen flux with the rate of olefin production at the surface of the membrane.

V. ACKNOWLEDGMENTS

This work was supported by the Fundamental Research Funds for the Central Universities (No.SWU113045 and No.XDJK2013C089).

[1] T. Niimi, H. Nagasawa, M. Kanezashi, T. Yoshioka, K. Ito, and T. Tsuru, J. Membr. Sci. **455**, 375 (2014).
[2] X. Liu, W. Z. Lang, L. L. Long, C. L. Hu, L. F. Chu, and Y. J. Guo, Chem. Eng. J. **247**, 183 (2014).
[3] T. T. Nguyen, L. Burel, D. L. Nguyen, C. Pham-Huu, and J. M. M. Millet, Appl. Catal. A **433**, 41 (2012).
[4] Z. T. Wu, I. M. D. Hatim, B. F. K. Kingsbury, E. Gbenedio, and K. Li, AIChE J. **55**, 2389 (2009).
[5] P. Botella, E. Garcia-Gonzalez, A. Dejoz, J. M. L. Nieto, M. I. Vazquez, and J. Gonzalez-Calbet, J. Catal. **225**, 428 (2004).
[6] F. Cavani, N. Ballarini, and A. Cericola, Catal. Today **127**, 113 (2007).
[7] S. Gaab, M. Machli, J. Find, R. K. Grasselli, and J. A. Lercher, Top. Catal. **23**, 151 (2003).
[8] K. Karim, A. Mamedov, M. H. Al-Hazmi, and N. Al-Andis, React. Kinet. Catal. Lett. **80**, 3 (2003).
[9] M. P. Lobera, S. Escolastico, and J. M. Serra, ChemCatChem **3**, 1503 (2011).
[10] E. Morales and J. H. Lunsford, J. Catal. **118**, 255 (1989).
[11] J. M. L. Nieto, P. Botella, P. Concepcion, A. Dejoz, and M. I. Vazquez, Catal. Today **91/92**, 241 (2004).
[12] R. K. Grasselli, Top. Catal. **21**, 79 (2002).
[13] P. Mars and D. W. van Krevelen, Chem. Eng. Sci. **3**, 41 (1954).
[14] V. Balcaen, I. Sack, M. Olea, and G. B. Marin, Appl. Catal. A **371**, 31 (2009).
[15] F. T. Akin and Y. S. Lin, J. Membr. Sci. **209**, 457 (2002).
[16] M. Rebeilleau-Dassonneville, S. Rosini, A. C. van Veen, D. Farrusseng, and C. Mirodatos, Catal. Today **104**, 131 (2005).
[17] H. H. Wang, Y. Cong, and W. S. Yang, Catal. Lett. **84**, 101 (2002).
[18] H. H. Wang, Y. Cong, and W. S. Yang, Chem. Commun. **14**, 1468 (2002).
[19] H. H. Wang, Y. Cong, X. F. Zhu, and W. S. Yang, React. Kinet. Catal. Lett. **79**, 351 (2003).
[20] Z. P. Shao, G. X. Xiong, H. Dong, W. H. Yang, and L. W. Lin, Sep. Purif. Technol. **25**, 97 (2001).
[21] M. Machli, C. Boudouris, S. Gaab, J. Find, A. A. Lemonidou, and J. A. Lercher, Catal. Today **112**, 53 (2006).

DOI:10.1063/1674-0068/27/06/690-696